Breakdown of the Coulomb friction law in TiC/a-C

Pei, Y. T.; Huizenga, P.; Galvan, D.; De Hosson, J. Th. M.

Published in:
Journal of Applied Physics

DOI:
10.1063/1.2396762

Publication date:
2006

Breakdown of the Coulomb friction law in TiC/*a*-C:H nanocomposite coatings

Y. T. Pei, P. Huizenga, D. Galvan, and J. Th. M. De Hosson[a)]
Department of Applied Physics, University of Groningen, Nijenborgh 4, 9747 AG Groningen, The Netherlands; The Netherlands Institute for Metals Research, P.O. Box 5008, 2600 GA Delft, The Netherlands; and The Materials Science Center, University of Groningen, Nijenborgh 4, 9747 AG Groningen, The Netherlands

(Received 28 July 2006; accepted 15 September 2006; published online 8 December 2006)

Advanced TiC/*a*-C:H nanocomposite coatings have been produced via reactive deposition in a closed-field unbalanced magnetron sputtering system (Hauzer HTC-1000 or HTC 1200). In this paper, we report on the tribological behavior of TiC/*a*-C:H nanocomposite coatings in which ultralow friction is tailored with superior wear resistance, two properties often difficult to achieve simultaneously. Tribotests have been performed at room temperature with a ball-on-disk configuration. In situ monitoring of the wear depth of the coated disk together with the wear height of the ball counterpart at nanometer scale reveals that the self-lubricating effects are induced by the formation of transfer films on the surface of the ball counterpart. A remarkable finding is a breakdown of the Coulomb friction law in the TiC/*a*-C:H nanocomposite coatings. In addition, the coefficient of friction of TiC/*a*-C:H nanocomposite coatings decreases with decreasing relative humidity. A superior wear resistance of the coated disk at a level of 10^{-17} m^3/N m (per lap) has been achieved under the condition of superlow friction and high toughness, both of which require fine TiC nanoparticles (e.g., 2 nm) and a wide matrix separation that must be comparable to the dimensions of the nanoparticles. © *2006 American Institute of Physics*. [DOI: 10.1063/1.2396762]

I. INTRODUCTION

The surface condition of a load-bearing component is usually the most important engineering factor. It is almost inevitably the outer surface of a workpiece that is subjected to wear and corrosion while it is in use. Since the time of Leonardo da Vinci (1452–1519), who was arguably the engineer to study friction and wear in detail, surface and coatings technology has become an important branch of modern surface science and engineering. Due to the complexity of wear processes combining individual physical events between sliding surfaces, it is still, however, a challenge to understand the precise mechanisms of friction and wear on the micrometer scale. Nevertheless, the economic aspects of friction and wear drive an increasing research effort in the development of coatings that might exhibit a combination of very low friction and low wear rates for applications in sliding and rolling contacts.

Friction between two surfaces in relative motion is a complex phenomenon that involves phonon dissipation, bond breaking and formation, strain-induced structural transformation and local surface reconstruction, and adhesion. From a physics point of view, it is determined by short- and long-range interactions between the surfaces and is often accompanied by wear. However, the underpinning mechanism of friction and the upscaling from atomic phenomena to microscopic effects are still not understood. The classical friction laws were discovered by da Vinci and Guillaume Amontons, respectively, and were summarized much later by Charles-Augustin Coulomb, who also contributed the third friction law. The three laws of friction describe that the friction force to resist sliding at an interface is (i) proportional to the normal force between the surfaces, (ii) independent of the apparent contact area, and (iii) independent of the sliding velocity. Recent research[1] has paid some attention to the effects of transfer films on friction behavior, but their importance is still rather overlooked.

The influence of environment on the friction of diamondlike carbon (DLC) based materials is a topic of controversy and remains under debate. Contradictory reports can be found of the effects of adsorbed gases on the friction coefficient. For example, Zaïdi *et al.* observed that the steady state coefficient of friction (CoF) of graphite fell as the partial pressure of oxygen gas increased or as the sliding velocity decreased.[2] In contrast, Heimberg *et al.* noted that adsorbed gases appeared to increase the CoF of hydrogenated DLC films.[3] Obviously, the surface characteristics of materials play a crucial role in the tribological performance.

In this paper, we report how and why the ultralow friction can be tailored and combined with superior wear resistance in advanced TiC/*a*-C:H nanocomposite coatings. The effects of the tribotesting condition and environment on the friction and wear rate of the coatings have been investigated. The results point to a breakdown of the Coulomb friction law.

II. EXPERIMENTS

Hydrogenated nc-TiC/*a*-C:H coatings were deposited by a closed-field unbalanced magnetron sputtering in an argon/acetylene atmosphere, using a Hauzer HTC-1000 or

a)Author to whom correspondence should be addressed; FAX: +31-50-363 4881 electronic mail: j.t.m.de.hosson@rug.nl

HTC-1200 coating system, configured with two Cr targets and two Ti targets, each pair being vertically opposed. The detailed setup of the coating system has been documented elsewhere.[4] The acetylene flow rate and substrate voltage bias were varied, each in the range of 80–125 SCCM (standard cubic centimeters per minute) and 0–150 V, respectively, to obtain different C/Ti ratios and nanostructures in the coatings. The coatings are named in such a way that the numbers preceding the character "V" indicate the substrate bias (in volts), and those following indicate the acetylene flow rate (in SCCM). The substrates used for each coating were $\phi 30 \times 5$ mm^2 disks of hardened M2 steel for tribological tests, 304 stainless steel for transmission electron microscopy (TEM) study, and $\phi 100$ mm Si wafer for microscopic observation of coating fracture cross sections and for residual stress measurements by monitoring the curvature change.

A calibrated MTS Nano Indenter XP was employed to measure the hardness (H) and Young's modulus (E) of the coatings with a Berkovich indenter. In order to obtain statistically reliable values of H and E, 30 indentations in total were configured, ten each on three different areas of each coating sample. The maximum indentation depth for measuring H and E was fixed at one-tenth of the coating thickness, namely, 150 nm. The averaged H and E values over the range of depth of 60–150 nm were taken as the hardness and modulus of a coating, with a typical standard deviation of 6%–10%.

Tribotests were performed at room temperature (20 ± 1 °C) on a CSM high-temperature tribometer with a ball-on-disk configuration at 5 N normal load and various sliding velocities. The resolution of the friction force measurement was ±0.3 mN in the measurement range of 0–20 N. In other words, the CoF measurement occurring was 10^{-4} or better at a normal load of 3 N or higher. The wear depth/height of the coated sample (disk) and the counterpart (commercial $\phi 6$ mm 100Cr6 bearing steel ball with hardness of HRC 60-62) was monitored *in situ* with a resolution of 0.02 μm by rotational variable differential transformer (RVDT) sensor during the tribotests, which allowed direct measurement of the thickness of the growing transfer film on the surface of the ball counterpart. The diameter of wear tracks was set in the range from $\phi 24$ to $\phi 18$ mm with a spacing of 1 mm between the tracks, so that a $\phi 30$ mm coated M2 steel disk was used four times. The set sliding velocities were attained by automatically varying the rotational speed of the disk samples according to the detected diameter of a wear track. Different levels of humidity were achieved by purging water vapor or dry air in the testing chamber at least for 5 H before a wear test. A confocal microscope was used to capture three-dimensional (3D) images on a wear track for measuring the wear volume and getting the wear rate.

The surface morphology and fracture cross sections of the coatings were examined using a scanning electron microscope (Philips FEG-XL30s). The investigation of the nanostructures was carried out in a high-resolution transmission electron microscope (HR TEM) (JEOL 4000 EX/II, operated at 400 kV). X-ray diffraction (XRD) scans were acquired using a Philips PW1877 diffractometer operating with a Cu $K\alpha$ radiation source placed at 1.5° incident angle to the coating surface. The average nanoparticle size in the different coatings was calculated from the full width at half maximum (FWHM) of the TiC (111) and TiC (200) peaks using the Scherrer equation. Electron probe microanalysis (EPMA) (Cameca SX-50) was used to determine the chemical composition of the coatings.

III. RESULTS

In a recently published paper we concluded that the microstructure of TiC/a-C:H nanocomposite coatings deposited by closed-field unbalanced magnetron sputtering system is influenced significantly by the substrate bias voltage and acetylene flow rate.[5] Undesirable columnar growth can be suppressed by increasing substrate bias voltage or carbon content, leading to the formation of a noncolumnar and substantial tougher microstructure. The appropriate substrate bias lies between 100 and 150 V; below the lower limit a columnar structure occurs and above the upper limit compressive stresses become so strong that the coating may delaminate from the substrate. Tribological tests have shown that the best combination of wear resistance and friction coefficient is obtained for the coatings of 80–90 at.% C content, confining the flow rate of acetylene in the range of 110–125 SCCM. As shown in Fig. 1(a), the columnar growth is fully suppressed in the coating 150V110 and TiC nanocrystallites are homogeneously embedded in the a-C:H matrix, with a mean particle spacing close to the size of the TiC nanoparticles [Fig. 1(b)]. In particular, self-lubricating effects have been clearly observed on the TiC/a-C:H nanocomposite coatings once the separation of TiC nanocrystallites in the a-C:H matrix is sufficiently wide. The wear tracks of the self-lubricating coatings are so smooth that they show almost no contrast and appear featureless, see Fig. 1(c). In this work we concentrate on the influence of various factors on the self-lubrication process.

A. Influence of sliding velocity on friction and wear

Figure 2 shows graphs of CoF versus laps for coatings 100V80 and 100V110, tested at different sliding velocities. The CoF graphs of coating 100V80 in Fig. 2(a) are nearly horizontal curves with large fluctuations, and the mean values of CoF at different velocities are almost the same, i.e., 0.218, 0.216, and 0.227 at different sliding velocities of 10, 30, and 50 cm/s, respectively. Apparently, the coating 100V80 without a self-lubricating effect exhibits a CoF that is independent of the sliding velocity. In other words, the Coulomb friction law holds in this case. In contrast, the CoF of coating 100V110 drops quickly from an initial high value of about 0.2 at the beginning of sliding to a very low value of CoF (<0.05) at the steady state, which is attributed to self-lubricating effects. Especially, a strong dependence of the steady state CoF on the sliding velocity is observed such that the faster the sliding velocity, the smaller the CoF [Fig. 2(b)]. The steady state CoF of coating 100V110 at sliding velocities of 10, 30, and 50 cm/s is 0.047, 0.030, and 0.013, respectively. It is clear that the Coulomb friction law is no longer valid when self-lubrication occurs.

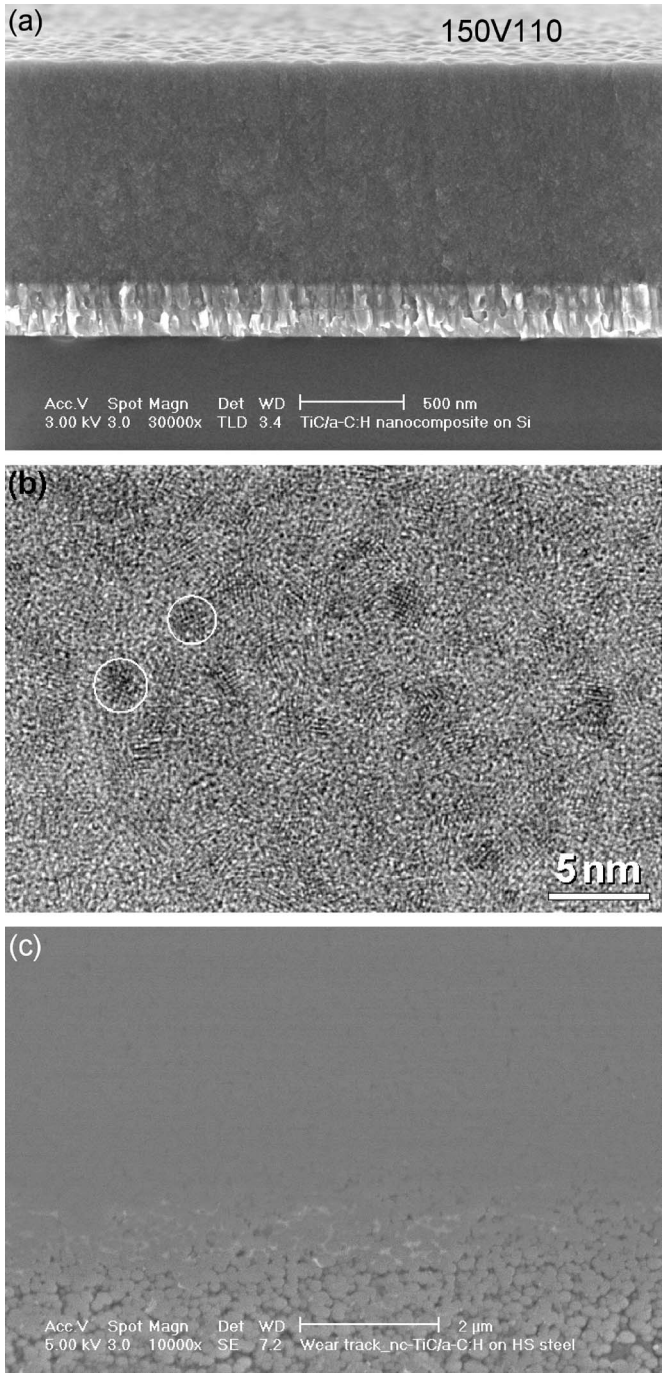

FIG. 1. (a) Scanning electron microscope (SEM) micrograph showing the fracture cross section of coating 150V110, (b) HRTEM micrograph revealing its nanostructure composed of TiC nanoparticles circled in white, and (c) smooth and featureless wear track (a part adjacent to the lower border of the track) on the coating formed in ball-on-disk tribotesting.

The phenomenon of reduced CoF as a function of increasing sliding velocity is not affected by relative humidity. Two groups of tribotests have been made on another self-lubricating coating (100V125) at relative humidities of 70% and 50%, respectively, and the results are displayed in Fig. 3. Although the CoFs of coating 100V125 are increased at the higher humidity, the overall dependence of CoF on sliding velocity is the same, that is to say, a lower CoF is observed at a faster sliding velocity, independent of the applied relative humidity. In addition, sometimes sharp jumps of CoF are

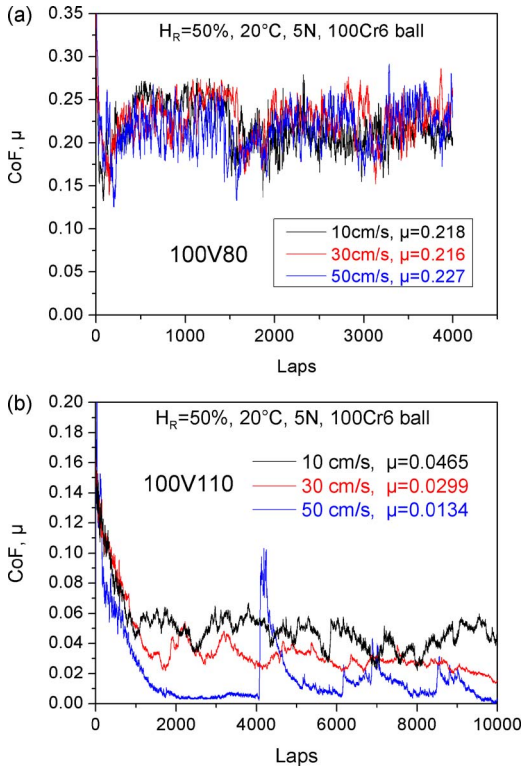

FIG. 2. Graph of coefficient of friction vs number of laps of the coatings: (a) 100V80 and (b) 100V110 under dry sliding against 100Cr6 steel ball.

observed at the highest sliding velocity of 50 cm/s (Figs. 2(b) and 3(b)). The typical shape of the CoF peaks, namely, a sudden jump followed by a long tail of decay, suggests a sudden removal of the transfer film at some critical accom-

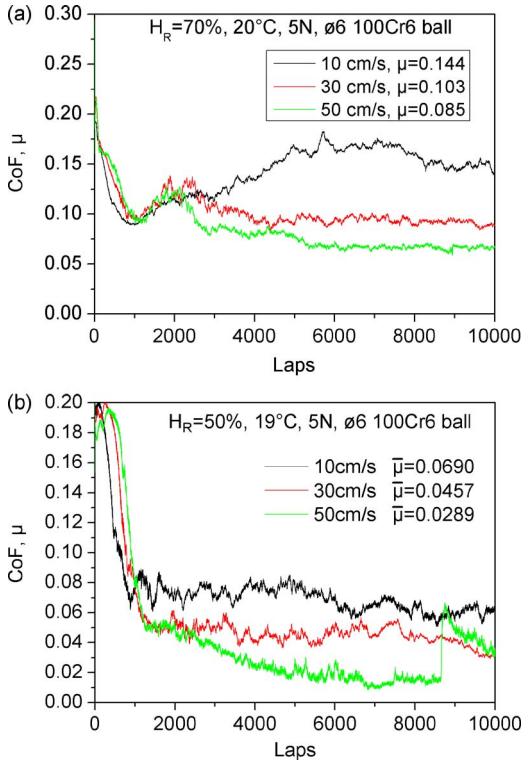

FIG. 3. Influence of sliding velocity on the CoF of coating 100V125 tested at different levels of relative humidity (H_R): (a) 70% and (b) 50%.

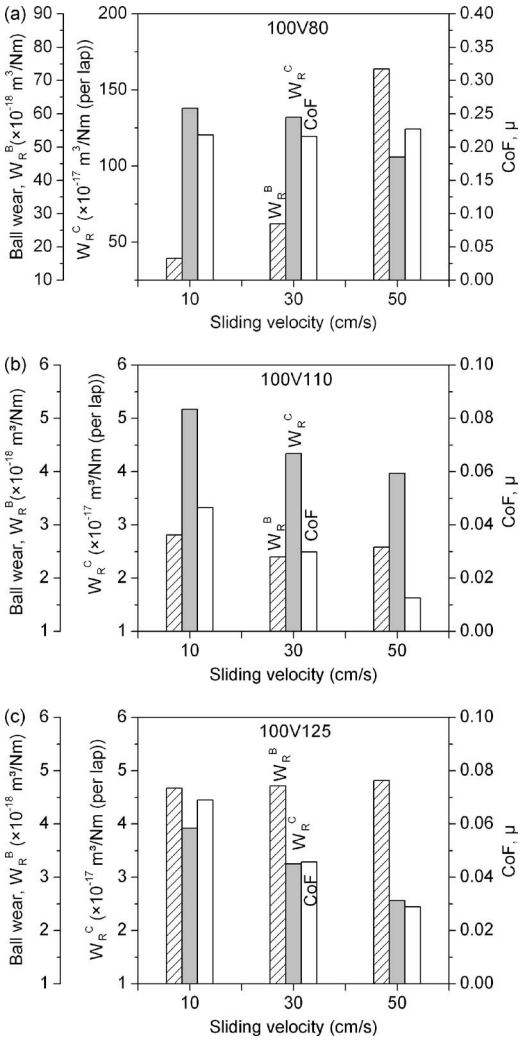

FIG. 4. Influence of sliding velocity on the wear rate of 100Cr6 ∅6 mm ball counterpart (W_{RB}) and the nanocomposite coatings (W_{RC}): (a) 100V80, (b) 100V110, and (c) 100V125 (5 N load, 50% relative humidity, and 20 °C room temperature). The steady state CoFs read from Figs. 2 and 3(b) are also plotted for better indication.

modated thickness followed by a new cycle of transfer film growth that gradually lowers the CoF to a steady state value again.[5] Such a breakdown of the transfer film at high sliding velocity may lead to a transition from a steady state situation to a metastable sliding condition that results in higher global CoF and wear rate values. There is therefore a limiting of dry sliding velocity at different levels of humidity, below which interrupted self-lubrication is retained, such that the CoF is stable and low. For instance, the critical velocities of coating 100V110, recorded at 0% and 50% relative humidities, were 10 and 50 cm/s, respectively. In general, sliding is limited to a lower velocity at low humidity, as we discuss in more detail in the next section.

The different frictional behavior of the nanocomposite coatings is directly reflected by the wear rate of the sliding couples. As shown in Fig. 4, the wear rate and CoF of coatings 100V110 and 100V125 obviously decrease with increasing sliding velocity, but the wear rate of the 100Cr6 ball counterpart stays almost constant. In contrast, coating 100V80 without self-lubrication demonstrates little reduction

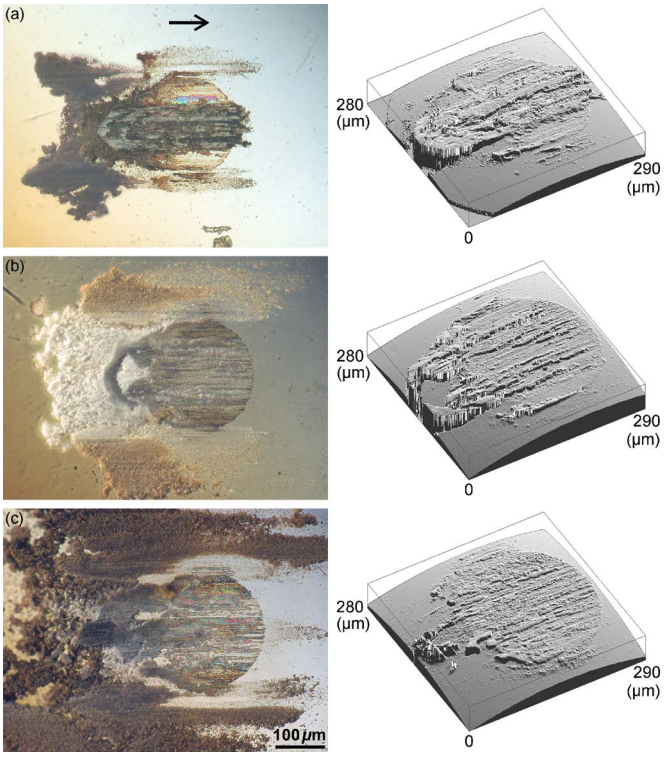

FIG. 5. Wear scar of 100Cr6 balls after sliding 10 000 laps against coating 100V125 under 5 N normal load, 70% relative humidity, and different sliding velocities: (a) 10 cm/s, (b) 30 cm/s, and (c) 50 cm/s. An arrow indicates the sliding direction of the coating in contact. The three-dimensional micrographs in the right column are captured with a confocal microscope after cleaning the wear debris and correspond to the two-dimensional (2D) optical micrographs in the left column.

in wear rate, but a significant increase in the wear rate of the 100Cr6 ball counterpart is seen with increasing sliding velocity, despite the CoF being independent of the sliding velocity.

Since self-lubrication is clearly a consequence of transfer film formation, it is important to examine the characteristics of transfer films formed under various testing conditions, such as their coverage, thickness, and density. The CSM tribometer automatically lifts up the loading arm at the end of a test, before the rotation of the disk sample slows down. In order not to disturb the status of the accumulated debris and transfer film on the ball counterpart surface, the counterpart, together with its holder, was carefully removed from the loading arm and put into an optical microscope for observation. Typical micrographs of the ball wear scars are shown in Fig. 5. A large amount of debris is accumulated in front and on the sides of the wear scars that are covered with transfer films. The colors of the debris and transfer films in the optical micrographs appear different because the assistant illumination for imaging was manually placed and varied among the experiments. Although the total amount of the debris accumulated differs among the three tests at different velocities (Fig. 5), the difference in the averaged amount of debris per unit sliding distance is not so significant because different diameters of wear tracks were used. The most significant difference among the three tests is the thickness of transfer films and the distribution of the debris around the wear scar. It is clearly revealed using the perspective three-

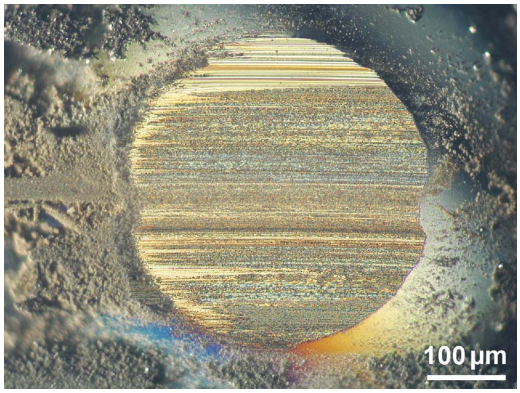

FIG. 6. Wear scar of 100Cr6 ball after sliding 10 000 laps against coating 100V80 under the tribotesting conditions of 5 N normal load, 10 cm/s sliding velocity, and 1% relative humidity.

dimensional confocal micrographs in Fig. 5 that the transfer films became thinner and looser at faster sliding velocity. In addition, the debris is stretched much farther from the wear scar at faster sliding velocity and a few debris were found in the narrow zone surrounding the scar [Fig. 5(c)]. This likely limits the flow of debris into the sliding contact and leads to a thin transfer film formed or even its breakdown under extreme conditions. We will discuss this item in more detail in the next section. In contrast, a thick ridge of transfer film is observed on the middle part of the wear scar in Fig. 5(a) and is spread evenly over the back border of the scar, which may explain the highest CoF measured at the slowest velocity and highest humidity [Fig. 3(a)].

Figure 6 shows the wear scar of 100Cr6 ball counterpart sliding against the coating 100V80. Dense and long scratches parallel to the direction of sliding are distributed over the whole scar, pointing to an abrasive wear mechanism. In particular, the front border of the scar is clearly visible and adjacent to a clean and bright margin that is not covered with any transfer film, which is rather different from the wear scar formed in sliding against the self-lubricating coatings as seen in Fig. 5. Besides the fact that the top bright part of the scar is exposed without a transfer film, the major dark region of the scar is actually covered by a large amount of individual debris particles embedded in the scratch grooves rather than by a continuous transfer film. Abrasive wear can, in this case, occur, since the coating is much harder than the ball (20 vs 7.5 GPa) and is composed of a high volumetric fraction (60%) of relatively large TiC nanoparticles that may act as the abrasive medium.

B. Effects of humidity on friction and wear

The effects of relative humidity on friction are demonstrated in Fig. 7(a). In general, the CoF of coating 100V110 decreases with decreasing humidity. Moreover, peaks have been recorded in the CoF curves when the relative humidity is equal to 25% or lower, and they occur more often in dry air if the sliding velocity stays constant. This implies that the sliding velocity used is close to the limit in dry air and also raises the steady state CoF slightly. These CoF peaks are attributed to the frequent breakdown of the transfer film as described above. Such a decrease of CoF with humidity has

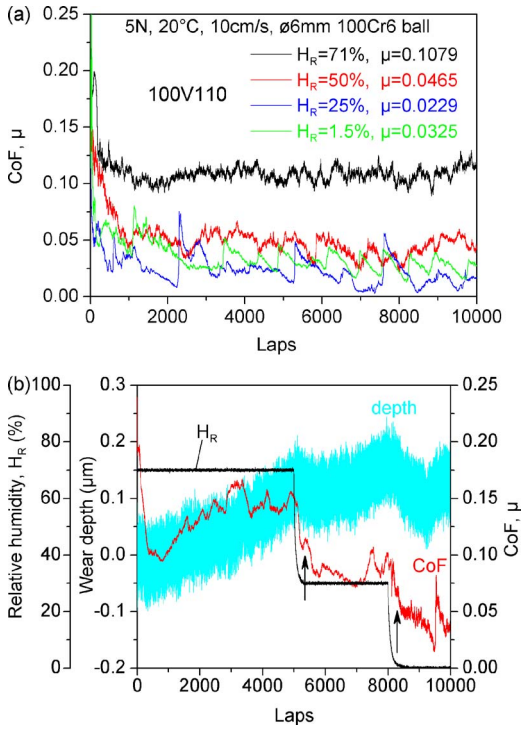

FIG. 7. (a) Effects of relative humidity on the CoF of coating 100V110 and (b) CoF dynamic response to humidity of coating 100V125.

also been observed for coating 100V125, where only a couple of peaks in the CoF curve occurred in dry air so that a monotonic decrease of CoF with decreasing humidity was recorded.[5] By comparing the frequency of the CoF peaks in dry air between coatings 100V110 and 100V125 [see Fig. 11(a) of Ref. 5], it should be pointed out that the critical sliding velocity is also affected by the volumetric fraction of *a*-C:H matrix: the wider the TiC particle separation in the matrix, the higher the critical velocity will be.

The dynamic response of CoF to humidity and the corresponding change in the transfer film thickness are shown in Fig. 7(b). Three levels of relative humidity, i.e., 70%, 30%, and 0%, were employed in a single tribotest run, where the transitions from high to low humidity were quickly realized by purging dry air into the testing chamber of the tribometer. During the first part of the tribotest at 70% relative humidity, the frictional behavior of coating 100V125 is just a replica of the results depicted in Fig. 3(a). It is interesting to note the change of CoF over the humidity transition periods. The CoF drops immediately once the humidity falls. Although the drop of CoF continues after the transition periods, there is a small step in the CoF decay corresponding to the end of the humidity drop, as marked by arrows in Fig. 7(b), after which the slope of the CoF drop is further reduced. This points to different mechanisms involved in the reduction of friction. Thickening of the transfer film starts immediately after the humidity drops, and lasts much longer than the transition periods, indicated by the segments of depth curve with a negative slope as shown in Fig. 7(b). Apparently, this thickening contributes to the whole course of the CoF drop. On the other hand, the thickness and coverage of adsorbed water molecular layer on the fresh transfer film and wear track are determined by the relative humidity and decrease as humid-

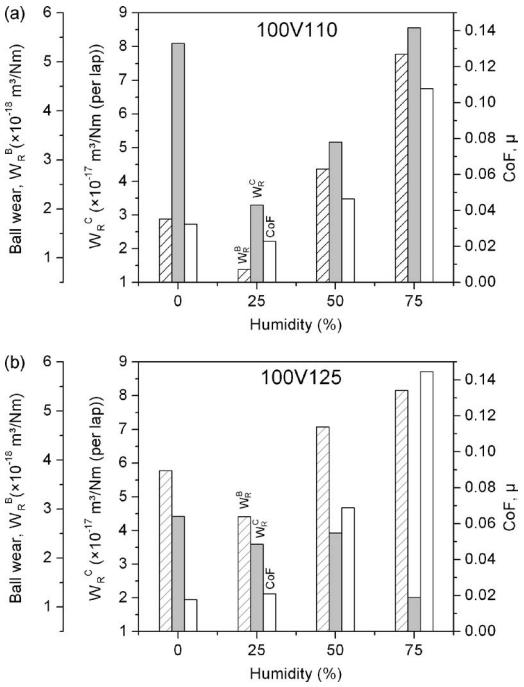

FIG. 8. Influence of humidity on the wear rate of 100Cr6 ball counterpart (W_{RB}) and coatings (W_{RC}) (a) 100V110 and (b) 100V125, tested at 5 N load, 10 cm/s sliding velocity, and 20 °C.

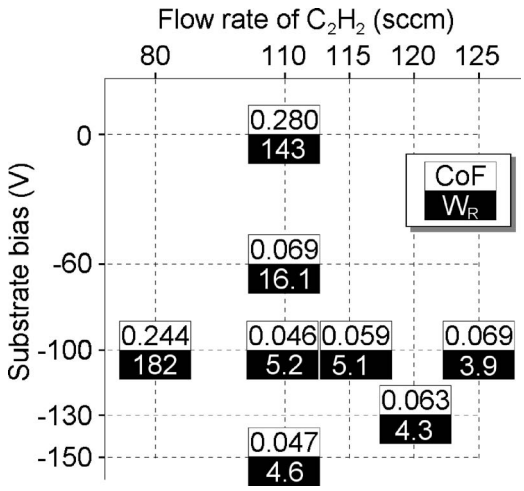

FIG. 9. Map of steady state CoF and wear rate (W_R) in dimension of $\times 10^{-17}$ m³/N m (per lap) vs the deposition parameters of TiC/*a*-C:H nanocomposite coatings under the same tribotesting conditions: H_R=50%, 20 °C, 5 N, 10 cm/s, sliding against ∅6 mm 100Cr6 ball.

ity lowers during the transition periods. It is understood that energy dissipation to the water molecular layer will accordingly decrease in the transition periods until a lower level is reached at lower humidity. This transition period is reflected in the first steep decline of CoF before the steps.

The two self-lubricating coatings exhibit a rather complicated wear response at different levels of humidity, as shown in Fig. 8. The wear rates of both the 100V110 coated disks and 100Cr6 ball counterpart decrease with decreasing humidity, with the exception in dry air where the wear rates and CoF increase [Fig. 8(a)]. This is attributed to the metastable status of wear in dry air as the sliding velocity is beyond the critical velocity, resulting in frequent transfer film breakdown and fluctuations in the degree of self-lubrication, as seen in Figs. 7(a) and 7(b). The wear rate of coating 100V125 at 75% humidity is obviously lower than that in dry air [Fig. 8(b)] and quite different from the situation of coating 100V110, although the CoF and the wear rate of the ball counterpart exhibit a similar evolution with humidity. It has to be realized that the high volumetric fraction of *a*-C:H matrix in coating 100V125 enhances the adsorption of water vapor to form quickly an adsorbed molecular layer on wear track surface after each ball pass. Such a rapidly formed layer of water molecules protects the coating from wear, but at the expense of higher friction. Another effect comes from the extra contribution of the enhanced toughness and high H/E ratio, discussed in the next section.

C. Trade-off between friction and wear resistance

The wear properties of TiC/*a*-C:H nanocomposite coatings versus deposition parameters are summarized in Fig. 9. Concerning the mechanical properties (Table I), it is clear that the wear rate (W_R) of the nanocomposite coatings decreases significantly with increasing H/E ratio and fracture toughness, but not with hardness (see also Table I). A high wear rate is always accompanied by a high coefficient of friction. The coefficient of friction decreases with increasing C content to a minimum value of 0.046 at 110 SCCM flow rate of acetylene, but increases again with further increase in C content (flow rate of acetylene). It is understood that the nanocrystalline TiC (nc-TiC) particles may serve as a promoter for surface graphitization of the *a*-C:H matrix that leads to ultralow friction. Surface graphitization of the *a*-C:H matrix is boosted due to the high localized shear stresses applied by the exposed nc-TiC in the transfer films (nanoscaled asperities). On the other hand, these TiC nanocrystallites also scratch the coating surface and facilitate wear. There is a trade-off between CoF and wear rate towards the low volume fraction of nc-TiC. It is thus understandable that the nanocomposite coatings exhibit even smaller CoFs, than those of pure DLC coatings (typically 0.1–0.15 under comparable conditions of loading and counterpart), where such hard and sharp nanoscaled TiC asperities (promoters) are missing. The importance of such a trade-off is that the coatings possessing various combinations of CoF and W_R can be selected for different applications according to whether high wear resistance or low friction is the major concern.

Although for a long time hardness has been regarded as a primary material property affecting wear resistance, the H/E ratio that we term the "elasticity index" is a more suitable parameter for predicting wear resistance, as originally proposed by Leyland and Matthews.[6,7] It is then reasonable to assume that wear resistance may be characterized by a power law dependence on H/E. This is so because the resistance to fracture (Irwin-Orowan-Griffith case) proceeds as a function of H^2/E, with the energy release rate proportional to the sqaure of the critical stress to failure, σ_c^2. A low elastic modulus will enhance the energy release rate and therefore the toughness. Likewise, the resistance of a (coated) surface to plastic deformation is proportional to H^3/E^2 because the yield pressure in a rigid ball contact on an elastic/plastic

TABLE I. Deposition parameters, composition, and properties of TiC/*a*-C:H nanocomposite coatings.

Coating code	Bias (−V)	C_2H_2 (SCCM)	Composition[a] (at. %) C	Ti	O	TiC V_F[b] (%)	*H* (GPa)	*E* (GPa)	*H*/*E*	Toughness (MPa·m$^{1/2}$)
0V110	Floating	110	71.34	13.64	15.02	27.7	5.5	61.3	0.090	···
60V110	60	110	80.21	16.33	3.46	29.5	11.8	99.8	0.118	23.66
100V110	100	110	81.02	17.84	1.14	31.7	15.6	136.6	0.114	36.15
150V110	150	110	80.30	18.51	1.19	33.1	19.8	168.3	0.118	49.94
100V80	100	80	66.60	31.75	1.65	60.1	20.0	229.4	0.087	32.21
100V125	100	125	87.19	11.85	0.96	19.7	15.8	128.5	0.123	55.78
100V115	100	115	83.50	15.34	1.16	26.7	14.8	124.5	0.119	···
130V115	130	115	83.12	16.02	0.86	28.0	17.4	146.9	0.118	43.13
130V120	130	120	85.42	13.72	0.86	23.4	17.4	140.1	0.124	51.68

[a]Excluding hydrogen.
[b]Providing 2.0 at. % saturation limit of Ti and 30 at. % H in the *a*-C:H matrix.

surface is a function of this ratio.[8] In Fig. 10 we have plotted the wear rates of the coatings versus the *H*/*E* ratio measured for each, showing curve fits based on either a power law function or an exponentionally decaying function of *H*/*E*. Both functionalities describe the experimental situation reasonably well, namely, that the wear rate decreases with increasing elasticity index of the coatings. For instance, coatings of high elasticity index such as 100V125 and 130V120 exhibit the highest wear resistance. The elasticity index essentially describes the capacity for elastic deformation before yielding plastically. Empirically, hardness is proportional to the yield stress of contact within a linear-elastic approach and, accordingly, a harder coating (assuming an identical elastic modulus) can bear higher loads before failing. More importantly, *H*/*E* is significant because a coating material with a lower Young's modulus can be expected to permit the redistribution of the applied load over a larger area, delaying failure of the coating/substrate system caused by high interfacial stresses. This is of particular importance in sliding and rolling contacts where alternating stress fields are developed, leading to surface fatigue in which the probability of crack initiation is exponentially proportional to the peak stress.

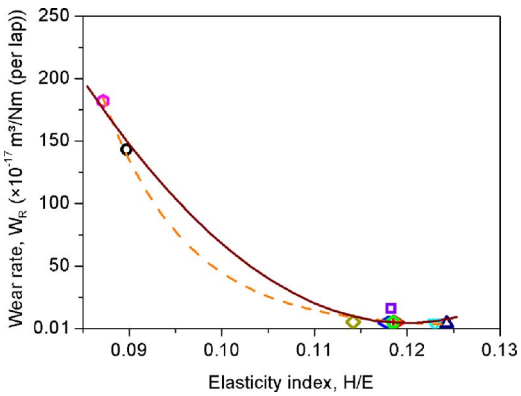

FIG. 10. Wear rate vs *H*/*E* ratio defined as the elasticity index of TiC/*a*-C:H nanocomposite coatings. The solid line represents a fit to a power law *H*/*E* dependence up to the second order and the dashed line is the fit to an exponentially decaying function in *H*/*E*. Each coating is represented by a different symbol: 0V110 (circle), 60V110 (square), 100V110 (diamond), 150V110 (left triangle), 100V80 (hexagon), 100V115 (right triangle), 100V125 (down triangle), 130V115 (pentagon) and 130V120 (up triangle).

Similarly, enhanced wear performance can be related to a high fracture toughness, the capability of adsorbing energy during crack propagation under surface fatigue of sliding or rolling contact.

IV. DISCUSSIONS

The self-lubricating effects of TiC/*a*-C:H nanocomposite coatings are induced by the formation of transfer films on the ball counterpart, which exhibit intrinsically low friction due to hydrogen passivation and graphitization of the amorphous hydrocarbon matrix. On the other hand, the dependencies of friction coefficient of the self-lubricating TiC/*a*-C:H nanocomposite coatings on sliding velocity and humidity are mainly a reflection of the tribological response of the *a*-C:H matrix to the testing environment. The effect of sliding velocity on CoF can be interpreted in terms of the exposure time required for ambient gases to interact with the surface of a wear track[3] and of the rheology of transfer films and associated wear debris.[2] The coverage/amount (q) of gas adsorption on a solid surface as a function of time (t) is commonly described by the Elovich equation:

$$\frac{dq}{dt} = Ae^{-\alpha q} \tag{1}$$

or its integrated form

$$q = \frac{1}{\alpha}\ln(\alpha A) + \frac{1}{\alpha}\ln\left(t + \frac{1}{\alpha A}\right), \tag{2}$$

where A is a constant related to the gas flux (or humidity in the case of water molecules under consideration here) and α is a constant associated with the number of available adsorption sites (related to the surface polarity of the hydrogenated *a*-C:H matrix). In ball-on-disk tribotests, each time the ball counterpart passes a point on the circular wear track, it "wipes" a contact area. Thereafter, the contact area is reexposed to gases in the environment for new adsorption; the exposure time between two successive wipes is inversely proportional to the sliding velocity. According to Eq. (1) the amount of adsorbed water molecules on the wear surface of the *a*-C:H matrix increases logarithmically with increasing humidity level and exposure time.

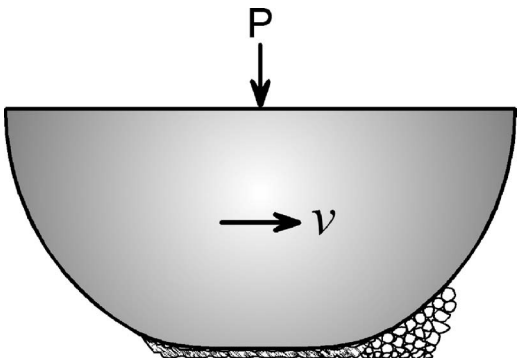

FIG. 11. Sketch of accumulated debris and transfer film on the wear scar of ball counterpart. The accumulated debris may collapse in low humidity or dry air beyond the critical sliding velocities, due to less densification at the absence of water molecules adsorbed.

A simple calculation based on the energy and force quantification between hydrogen and carbon atoms has revealed that the repulsive force of *a*-C:H surface acting on C–H bonds could decrease to a value two orders of magnitude lower than that of vacuum conditions.[9] Therefore, small quantities of adsorbed water vapor can inhibit the desorption of atomic hydrogen and, consequently, the passivation of newly broken C bonds, leading to an increase in the coefficient of friction. On the other hand, water molecules easily interact with the hydrophilic surface of the steel ball counterpart. Extra work must be expended to break the interatomic bonds between the adsorbates and sliding interfaces.

The transfer film and the wear debris accumulated in front of the wear scar of the ball counterpart actually carry the contact load, as sketched in Fig. 11; their rheology is of prime importance in lowering friction. When this nanosized debris is (in dry air) not covered by water molecules, it may be brought into (and easily sheared at) the sliding interfaces with a very weak interaction between both themselves and the surface of the wear track. However, at high sliding velocity the flow of debris into the sliding contacts may be interrupted due to the collapse of accumulated debris in front of the wear scar. Such collapses lead to the frequent breakdown of transfer films and, correspondingly, to the peaks of CoF beyond the critical sliding velocity, see Fig. 7(a). At faster sliding velocity and/or lower level of humidity, the films become thinner and looser and therefore they easily break. Collapses of the accumulated debris are expected to be more damaging to the thinner transfer films seen at higher sliding velocities. Condensation of water molecules collected from the surface of the wear track may change the nature of transfer films in humid air. It is well known that adsorbed gases, especially water vapor, increase the rate of densification of particulate materials, for instance, wear debris accumulated here. As seen in Fig. 5(a), denser and thicker transfer films have been formed at higher humidity and at slower velocity. One can conclude that it requires more energy expenditure (as friction) to slide and smear such a film than a loose and easy shearing one between the sliding surfaces.

As a general trend, lower friction accompanies a lower wear rate of TiC/*a*-C:H nanocomposite coatings, as seen in Figs. 4 and 8(a). Coating 100V125 is an exception that exhibits lower wear rate together with a higher CoF in higher humidity. It should be pointed out that the coating possesses the highest fracture toughness due to its optimized nanostructure, where the separation width of *a*-C:H matrix is close to the size of TiC nanocrystallites, resulting in much higher resistance against surface fatigue and thus better wear resistance. Fewer amounts of TiC nanoparticles contained in the transfer film also produce less scratching on the wear track surface, which is covered more by adsorbed water molecules. In other words, less material can be removed during wear.

In the case of nonlubricating coatings such as 100V80 where the Coulomb friction law holds, the wear rate of 100Cr6 ball counterparts increases significantly with sliding velocity, in contrast to the wear rate of the coating itself. This is mainly attributed to the thermal response of the wear couple (100Cr6 bearing steel and the nanocomposite coating) to the flash temperatures in the sliding contact. Although many models and theoretical considerations on the flash temperatures have been proposed during the past decades since Blok's,[10–12] experimental validations of the models are still very difficult. In general, the flash temperature (ΔT) can be described as a function of sliding velocity (v):[13]

$$\Delta T = \frac{1}{4}\frac{\mu P v}{(K_1 + K_2)a}, \tag{3}$$

where μ is the CoF, P the applied normal load, K_1 and K_2 the thermal conductivities of the ball counterpart and the coating, and the radius of the real contact area $a=(P/\pi H)^{1/2}$, with H the hardness of the softer material between the coating and the counterpart. Therefore, the temperature rise of the protuberances in the sliding contact induced by friction is linearly proportional to the sliding velocity and the CoF. It thus clarifies that higher flash temperatures result from a faster sliding velocity and also from the higher value of constant CoF observed on the nonlubricating coatings, in comparison with the ultralow CoF of the self-lubricating coatings. A rough estimate based on the employed conditions of tribological tests and the physical properties of the materials ($K_1=17$ W m^{-1} K^{-1}, $K_2=13.8$ W m^{-1} K^{-1} for the coating 100V80 of 60 vol % TiC nanocrystallites and $a=14.4$ μm) indicates that the flash temperatures are 62, 183, and 320 °C at sliding velocities of 10, 30, and 50 cm/s, respectively. It is known that 100Cr6 bearing steels start to soften at temperatures typically between 180 and 190 °C.[14] Accordingly, the asperities on the wear scar of the 100Cr6 ball start to thermally yield at the sliding velocity of 30 cm/s and heavily yield at 50 cm/s. It can be concluded that thermal yielding of the asperities beyond the softening temperature leads to a significant increase in the wear rate of the 100Cr6 ball counterpart as the flash temperature becomes higher with increasing sliding velocity. Our recent work showed that TiC/*a*-C:H nanocomposite coatings are thermally stable up to an annealing temperature of 350 °C, with a reduction of less than 10% in hardness after annealing for 1 h at 350 °C in air.[15] In view of this, a change in the coating's wear status is not expected when the flash temperature is below its softening temperature. Particularly, in tribological tests of "ball-on-disk" configuration, the wear scar of the ball is continuously in contact with the coating, whereas the corresponding areas

on the coating sample are only once in periodic contact during each disk revolution. This implies that the asperities on the wear scar of the ball counterpart undergo continuous thermal loading at the flash temperature, but those on the wear track of the coating only bear a pulsed thermal loading once per disk revolution from which they can recover between cycles. This makes a large difference in thermal fatigue of the asperities in the sliding contact of the wear couple. Such a dependence of the wear rate of the ball counterpart on the sliding velocity has not been observed with the self-lubricating coatings within the maximum sliding velocity used, because the CoF is nearly ten times smaller. It results in a much lower flash temperature that is far below the softening temperature of the 100Cr6 bearing steel. In addition, the wear scar of the ball is actually covered by the transfer films that act as solid lubricants and protect the scar to a great extent from wear.

V. CONCLUSIONS

TiC/*a*-C:H nanocomposite coatings of optimal nanostructure exhibit strong self-lubricating effects, combining ultralow friction with superior wear resistance. The results of tribological investigations point to a breakdown of the Coulomb friction law in the case of self-lubricating TiC/*a*-C:H nanocomposite coatings, namely, a lower coefficient of friction (CoF) at faster sliding velocity. The CoF of the self-lubricating coatings decreases with decreasing relative humidity. There is a trade-off between CoF and wear rate towards the low volume fraction of nc-TiC, the significance of which is that coatings with various combinations of CoF and W_R can be selected for different applications according to whether high wear resistance or low friction is the primary requirement. Physical arguments have been proposed to explain and better understand the friction and wear phenomena observed for such coatings.

ACKNOWLEDGMENTS

The authors acknowledge financial support from the Netherlands Institute for Metals Research (NIMR) and the Foundation for Fundamental Research on Matter (FOM-Utrecht). C. Strondl from Hauzer Techno Coating BV, The Netherlands, is acknowledged for his help with the deposition of the coatings.

[1] I. L. Singer, Langmuir **12**, 4486 (1996).
[2] H. Zaïdi, D. Paulmier, and J. Lepage, Appl. Surf. Sci. **44**, 221 (1990).
[3] J. A. Heimberg, K. J. Wahl, I. L. Singer, and A. Erdemir, Appl. Phys. Lett. **78**, 2449 (2001).
[4] C. Strondl, N. M. Carvalho, J. Th. M. De Hosson, and G. J. van der Kolk, Surf. Coat. Technol. **162**, 288 (2003).
[5] Y. T. Pei, D. Galvan, and J. Th. M. de Hosson, Acta Mater. **53**, 4505 (2005).
[6] A. Leyland and A. Matthews, Wear **246**, 1 (2000).
[7] A. Leyland and A. Matthews, Surf. Coat. Technol. **177–178**, 317 (2004).
[8] T. Y. Tsui, G. M. Pharr, W. C. Oliver, C. S. Bhatia, R. L. White, S. Anders, A. Anders, and I. G. Brown, Mater. Res. Soc. Symp. Proc. **383**, 447 (1995).
[9] T. Le Huu, H. Zaïdi, and D. Paulmier, Wear **181–183**, 766 (1995).
[10] H. Blok, Proc. Inst. Mech. Eng. **2**, 222 (1937).
[11] F. P. Bowden and P. H. Thomas, Proc. R. Soc. London, Ser. A **223**, 29 (1954).
[12] X. F. Tian and F. E. Kennedy, J. Tribol. **116**, 167 (1994).
[13] E. Rabinowicz, *Friction and Wear of Materials*, 2nd Ed. (Wiley, New York, 1965), pp. 86–90; (Wiley, New York, 1995), pp. 99 and 100.
[14] P. Daguier, G. Baudry, J. Bellus, G. Auclair, J. Rofès-Vernis, G. Dudragne, D. Girodin, and G. Jacob, in *Bearing Steel Technology*, Proceedings of the Sixth International Symposium on Bearing Steels, edited by J. M. Beswick (American Society for Testing Materials, West Conshohocken, PA, 2001).
[15] Y. T. Pei, D. Galvan, and J. Th. M. de Hosson, J. Vac. Sci. Technol. A **24**, 1448 (2006).